J. Appl. Geophys., Vol. 5, March 2006, 379-396.

ATTENUATION PROPERTIES OF THE UPPER CRUST IN EASTERN AND SOUTHERN ARABIA FROM SURFACE WAVES

By

T. A. Mokhtar

Department of Geophysics, Faculty of Earth Sciences, King Abdulaziz University.

P.O. Box 80206, Jeddah 21589, Kingdom of Saudi Arabia.

ABSTRACT

Regionalized Rayleigh and Love wave's attenuation coefficients for the upper crust have been determined across the Eastern Arabian Plate and the Southern Arabian Plate regions, using data from events in Western Iran and the Gulf of Aden recorded by RAYN station. RAYN is located in the middle part of the Arabian plate. The method of frequency ratio was applied and Q_{β}^{-1} models were inverted through using the measured attenuation coefficients for both regions, then Q_{α}^{-1} models are determined from the inverted Q_{β}^{-1} models.

In general, it is found from the results of this study that surface waves attenuation in the upper crust of the Southern Arabian Plate Region (SAPR) is higher than that of the Eastern Arabian Plate Region (EAPR). The average Q_{β} in the upper 10 km of the crust is found to be 56 and 40 in EAPR and SAPR, respectively. Crustal Q_{β} for the upper 25 km are 94 and 70 for the EAPR and SAPR, respectively.

The high attenuation of the upper crust of the Arabian plate is attributed mainly to the ongoing tectonic processes in the Red Sea, in which it reflects the effect of high heat flow associated with it. Fluid motion through cracks and faults in the upper crust provides the best mechanism for explaining the low Q_{β} in the southern region of the plate, while the presence of a thick sedimentary cover in the upper crust is the main cause of high attenuation of surface waves in the eastern region of the plate. The high surface waves attenuation values in the upper crust of the Southern Arabian Plate region, as correlated with those of the Eastern Arabian Plate region can be explained by the proximity of the former region to the ongoing tectonic activities in the Southern Red Sea and the Gulf of Aden regions.

hydration, at depth in the crust. He suggested that, the temperature may indirectly contribute to regional Q variations in the upper crust, if hydrothermal reactions are involved.

The region of South and Southwestern Arabia is adjacent to the tectonically and seismically active regions (Ambraseys et al., 1994). Northern Yemen was subjected to a magnitude 6.0 (Ms and m_b) earthquake on 13, 1982. Studying the hypocentral locations of 230 aftershocks, following the 1982 event, with duration magnitudes between 1.8 and 4.6, Langer et al. (1987) presented evidences from composite focal mechanism of these events that pointed to the presence of a graben structure composed of normal faults with northwest strikes. The strikes of the faults are parallel to the main axis of the Red Sea central graben and are indicative of tensional stresses acting on the southwest of the Arabian Plate.

Heat flow measurements at shot points along the 1978 Saudi Arabian deep seismic refraction profile, that extends to the southwest along 1000 km from west of Riyadh to the Farasan Islands, showed an increase in heat flow toward the Red Sea margin (Gettings and Showail, 1982). The high heat flow at the shot points located at the southwestern end of the profile along the Red Sea margin was explained by heating from the abutting oceanic crust and/or an enhanced mantle component of heat flow through the thin continental crust. In the actively spreading axial trough, classical sea-floor spreading models, that allow for hydrothermal convective activity are adequate to explain the observed heat flow (Gettings, 1982).

In the eastern platform region, the attenuation of seismic surface waves in the upper crust is less than that in the southern and southwestern Arabian plate region. However, it is higher than other regions of the world. Q_β in this region is about 65-85 (Seber and Mitchell, 1992). These low values are difficult to explain in terms of the tectonic process taking place in the Red Sea. It is possible that, the high attenuation in this area is due to the presence of thick sedimentary cover in the upper crust of the Eastern and Southeastern Arabian Peninsula. The total sedimentary thickness reaches about 6000m and depths to the base of the Mesozoic sediment reach 4500 m in that region (Brown, 1972).

The method of frequency ratio, used by Mokhtar (1996), was applied in this study to determine the surface waves attenuation coefficients for both Rayleigh and Love waves. Q_β^{-1} models were inverted through using the measured attenuation coefficients for both SAPR and EAPR regions, and Q_α^{-1} models were determined from the inverted Q_β^{-1} models.

In general, it is found from the results of this study that, surface waves attenuation in the upper crust of SAPR is higher than that of EAPR. The average Q_β in the upper 10 km of the crust is found to be 56 and 40 in EAPR and SAPR, respectively. Crustal Q_β for the upper 25 km are 94 and 70 for the EAPR and SAPR, respectively.

The results of the present study are consistent with the ideas of Mitchell (1975) and the laboratory studies of Q at crustal temperature and pressure. Thus, it appears that, fluid motion through cracks and faults in the upper crust provides the best mechanism for explaining the low Q in the Southern and Southwestern Arabian plate region, as compared to the relatively higher Q values in the upper crust of the Eastern Arabia.

Acknowledgments

The author would like to express his thanks to the (IRIS/IDA) IRIS GSN/ UNIVERSITY of California San Diego, for providing the data of Ar Rayn (Saudi Arabia) through IRIS.

REFERENCES

Ambraseys, N. N., C. P. Melville, and R. D. Adams (1994). *The Seismicity of Egypt, Arabia and the Red Sea, a historical review.* Cambridge University Press, 181 P.

Anderson, D. L., A. Ben-Menahem and C. B. Archambeau (1965). Attenuation of seismic energy in the upper mantle, *J. Geophys. Res.*, 70, 1441-1448.

Brown, G. F. (1972). Tectonic map of the Arabian peninsula, U.S. Geol. Surv.

Chen, J. J. (1985). Lateral variation of surface wave velocity and Q structure beneath North America, *Ph. D.* dissertation, Saint Louis Univ., St. Louis, Mo., U.S.A.

Cheng, C. C., and B. J. Mitchell (1981). Crustal Q structure in the United States from multimode surface waves, *Bull. Seismol. Soc. Am.*, 71, pp. 161-181.

Cong , L., and B. J. Mitchell (1998). Seismic velocity and Q structure of the Middle Eastern crust and upper mantle from surface-wave dispersion and attenuation, *Pure appl. Geophys* , 153, pp. 503-538.

Gettings, M. E(1982). Heat-flow measurements at shot points along the 1978 Saudi Arabian seismic deep-refraction line, Part 2--Discussion and interpretation: Saudi Arabian Deputy Ministry for Mineral Resources Open-File Report USGS-OF-02-40, 40 P.

Gettings, M. E. and A. Showail (1982). Heat flow measurements at shot points along the 1978 Saudi Arabian deep-refraction line, Part I. Results of measurements. Saudi Arabian Dir. Gen. Miner. Resour. Open-file Rep. 02-39, 98 P.

Ghalib, H. (1992). Seismic velocity structure and attenuation of the Arabian plate. Ph. D. Dissertation, St. Louis University, St. Louis, Missouri, USA, 314 P.

Housley, R. M., B. R. Tittmann, and E. H. Cirlin (1974). Crustal porosity information from internal friction profile, *Bull. Seism. Soc. Am.*, 64, pp. 2003-2004.

Langer, C. J., G. A. Bollinger, and H. M. Merghelani (1987). Aftershocks of the 13 December 1982 North Yemen earthquake: Conjugate normal faulting in an extensional setting, *Bull. Seismol. Soc. Am.*, 77, 6, pp. 2038-2055.

Lee, W. B., and S. C. Solomon (1975). Inversion schemes for surface wave attenuation and Q in the crust and upper mantle, *Geophs. J. R. astr. Soc.*, 43, pp. 47-71.

Lee, W. B., and S. C. Solomon (1978). Simultaneous inversion of surface wave phase velocity and attenuation: Love waves in western North America, *J. Geophys. Res.*, 83, pp. 3389-3400.

Mitchell, B. J. ,1975. Regional Rayleigh wave attenuation in North America, *J. Geophys. Res.* , 80, pp. 4904-4916.

Mitchell, B. J., N. K. Yacoub, and A. C. Correig (1977). A summary of seismic surface wave attenuations and its regional variations across continents and oceans, in: The Earth Crust, *Am. Geophs. Union Monograph*, 20, Washington, D. C.

Mitchell, B. J., 1980 Frequency dependence of shear wave internal friction in the continental crust of eastern North America, *J. Geophs. Res.*, 85, pp. 5212-5218.

Mokhtar, T. A., 1987. Seismic velocity and Q model for the shallow structure of the Arabian Shield from short period Rayleigh waves, *Ph. D. Thesis*, Saint Louis University, Saint Louis, Missouri, U.S.A., 168 P.

Mokhtar, T. A., 1995. Phase velocity of the Arabian platform and its attenuation characteristics by wave-form modeling. *J. King Abdulaziz Univ. Earth Sci.* 8, pp. 23-45.

Mokhtar, T. A., 1996. Surface wave attenuation in the Arabian plate. Egypt. J. Geol., 40-2, pp. 695-719.

Mokhtar, T. A., 2004. Variations of the Crustal Structure of Arabia. *Journal of King Abdulaziz University, Earth Sciences*, vol. 15, pp. 1-27.

Mokhtar, T. A., (2006). Surface Waves Anelastic Attenuation Beneath Southwest of the Arabian Peninsula and the Southern Red Sea. *Journal of King Abdulaziz University, Earth Sciences*, in press.

Mokhtar, T. A., R. B. Herrmann, and D. R. Russell, 1988. Seismic velocity and Q model for the shallow structure of the Arabian shield form short period Rayleigh waves, *Geophysics*, 53, pp. 1379-1387.

Mokhtar, T. A., and Al-Saeed, M. M. 1994. Shear wave velocity structures of the Arabian Peninsula, *Tectonophysics*, 230, pp. 105-125.

Mokhtar, T. A., C. J. Ammon, R. B. Herrmann, and H. A. A. Ghalib (2001). Surface wave velocities across Arabia, *Pure and Applied Geophysics*, 158, pp. 1425-1444.

Seber, D. and B. Mitchell (1992). Attenuation of surface waves across the Arabian peninsula, *Tectonophysics*, 204, pp. 137-150.

Yacoub, N. and B. J. Mitchell (1977). Attenuation of Rayleigh wave amplitudes across Eurasis, *Bull Seism. Soc. Am.*, 67, pp. 751-769.

Wiggins, R. A. (1972). The general linear inverse problems implication of surface waves and free oscillations for earth structure, *Rev. Geophys. Space Phys.*, 10, pp. 251-285.

Winkler, K. and A. Nur (1979). Pore fluids and seismic attenuation in rocks, *Geophys. Res. Letters*, 6, pp. 1-4.

Winkler, K. and A. Nur (1982). Pore Seismic attenuation: Effects of pore fluids and frictional sliding. , *Geophysics*, 47, pp. 1-15.

Table (1)

No.	DATE YYYY/MM/DD
1	1997/04/19
2	1997/04/21
3	1997/05/26
4	1997/06/02
5	1997/07/27
6	1997/07/27
7	1997/08/14
8	1997/08/29
9	1997/08/29
10	1997/10/03
11	1997/10/23
12	1997/11/18
13	1998/12/11
14	1998/01/11
15	1998/01/15
16	1998/01/17
17	1998/01/18
18	1998/01/19
19	1998/06/13
20	1998/06/15
21	1998/10/29
22	1998/11/08
23	1998/11/12
24	1998/11/14
25	1998/11/15
26	1998/12/09
27	1998/12/10
28	1999/01/15
29	1999/03/10
30	1999/03/29
31	1999/04/28
32	1999/04/30
33	1999/04/30
34	1999/05/16
35	1999/05/21
36	1999/05/30
37	1999/06/22
38	1999/09/13
39	1999/09/25
40	1999/09/27
41	1999/12/09
42	1999/12/23
43	1999/12/25
44	2000/01/17
45	2000/02/10
46	2000/03/11
47	2000/03/13
48	2000/04/12
49	2000/07/06
50	2000/09/08
51	2000/09/11
52	2000/09/13

Appendix

Table (1) Earthquake epicenteral data for events located in Western Iran

No.	DATE	ORIGIN TIME	LATITUDE°	LONGITUDE°	DEPTH	Mb	Ms
	YYYY/MM/DD	HH:MM:SS.SS			(km)		
1	1997/04/19	22:31:37.5	27.943	56.869	22	4.8	4.6
2	1997/04/21	17:12:44.9	27.906	56.860	20	4.7	
3	1997/05/26	01:17:54.0	32.937	47.035	33	4.7	
4	1997/06/02	03:54:42.9	33.963	48.291	27	4.7	
5	1997/07/27	01:59:30.8	29.141	52.304	33	4.6	
6	1997/07/27	23:33:25.8	27.527	56.644	33	4.9	4.7
7	1997/08/14	19:38:26.2	29.059	51.537	33	4.7	4.0
8	1997/08/29	14:43:57.4	27.562	55.888	33	4.8	4.2
9	1997/08/29	15:55:59.8	27.192	53.902	33	4.6	
10	1997/10/03	17:01:00.8	27.761	54.709	33	4.8	4.1
11	1997/10/23	14:35:32.8	28.043	53.870	33	4.8	4.1
12	1997/11/18	06:56:57.5	33.052	48.083	33	4.6	
13	1998/12/11	00:58:15.9	28.283	55.535	33	4.9	
14	1998/01/11	08:08:05.9	30.500	50.630	33	4.7	
15	1998/01/15	04:00:51.4	26.281	55.391	33	4.6	
16	1998/01/17	05:21:35.2	32.574	48.103	33	4.7	
17	1998/01/18	03:12:50.9	30.467	50.531	33	4.8	
18	1998/01/19	22:08:57.8	33.745	46.906	33	4.8	
19	1998/06/13	02:23:43.8	27.785	53.690	33	4.6	3.8
20	1998/06/15	01:14:35.9	31.712	50.835	31	4.9	4.8
21	1998/10/29	20:57:27.6	31.850	48.792	33	4.6	
22	1998/11/08	19:50:38.7	29.571	51.324	33	4.8	
23	1998/11/12	15:36:10.7	33.224	49.708	33	4.8	
24	1998/11/14	10:37:23.2	27.887	53.550	47	4.7	
25	1998/11/15	20:30:21.4	27.127	55.543	33	4.6	
26	1998/12/09	09:25:03.3	31.075	49.643	33	4.6	
27	1998/12/10	14:21:50.8	27.845	53.517	33	4.7	
28	1999/01/15	13:46:09.7	35.515	45.196	33	4.7	
29	1999/03/10	07:45:43.4	28.868	56.595	85	4.8	
30	1999/03/29	04:00:39.0	29.611	51.493	33	4.7	4.1
31	1999/04/28	18:11:43.6	27.808	53.536	33	4.7	
32	1999/04/30	04:20:02.5	27.837	53.538	36	4.9	4.8
33	1999/04/30	14:54:22.0	35.968	45.653	33	4.6	
34	1999/05/16	23:36:01.5	29.402	52.043	33	4.6	
35	1999/05/21	19:17:43.6	29.555	51.899	33	4.6	
36	1999/05/30	00:15:40.6	29.476	51.967	58	4.6	3.9
37	1999/06/22	17:04:51.6	29.316	51.978	33	4.6	
38	1999/09/13	23:32:07.7	31.907	50.590	33	4.8	4.3
39	1999/09/25	19:19:30.0	28.711	51.208	33	4.7	4.9
40	1999/09/27	02:31:24.5	28.650	51.284	33	4.6	
41	1999/12/09	17:04:04.4	27.605	54.191	33	4.7	
42	1999/12/23	03:07:31.4	29.493	51.820	55	4.7	
43	1999/12/25	03:07:49.3	33.304	47.150	33	4.7	
44	2000/01/17	16:39:50.09	27.508	54.314	33	4.6	
45	2000/02/10	01:26:19.96	28.824	54.896	33	4.8	4.5
46	2000/03/11	07:08:33.02	28.673	51.346	33	4.6	
47	2000/03/13	23:16:19.09	29.204	51.440	33	4.7	
48	2000/04/12	08:20:13.69	32.919	49.461	33	4.7	
49	2000/07/06	08:34:29.11	30.120	51.724	52	4.7	
50	2000/09/08	05:22:40.88	30.610	49.790	33	4.7	3.8
51	2000/09/11	16:54:56.52	35.713	45.206	33	4.6	
52	2000/09/13	03:55:11.12	27.762	51.735	33	4.7	4.0

Table (1) (continue)

No.	DATE	ORIGEN TIME	LATITUDE	LONGITUDE	DEPTH	Mb	Ms
	YYYY/MM/DD	HH:MM:SS.SS			(km)		
53	2000/09/13	09:04:23.25	27.705	51.749	33	4.7	
54	2000/10/13	21:12:06.48	30.698	49.681	33	4.7	3.9
55	2000/12/21	10:39:48.49	26.636	55.706	33	4.7	4.0
56	2001/01/01	05:14:05.69	27.426	52.954	33	4.6	
57	2001/02/13	03:42:40.21	28.122	56.343	33	4.6	
58	2001/02/22	03:19:58.11	29.369	51.938	33	4.9	
59	2001/03/21	20:31:13.50	27.077	53.811	33	4.6	
60	2001/04/13	04:57:16.48	28.229	54.862	33	4.6	
61	2001/04/24	20:13:09.53	29.459	51.965	33	4.6	
62	2001/05/23	14:51:13.26	29.901	51.230	33	4.7	
63	2001/06/09	04:45:33.46	29.454	52.190	33	4.6	
64	2001/10/25	21:34:48.27	32.651	47.972	100	4.6	
65	2001/11/17	12:14:46.90	30.452	50.451	33	4.7	
66	2002/02/20	10:12:29.52	33.738	45.648	33	4.9	
67	2002/02/23	17:09:36.31	26.853	54.752	33	4.6	
68	2002/03/02	22:12:57.26	32.801	48.186	33	4.8	
69	2002/03/09	15:43:23.19	28.104	51.669	33	4.6	
70	2002/04/04	15:44:32.18	27.062	55.244	16	4.8	
71	2002/04/08	16:34:06.91	27.106	55.231	59	4.8	
72	2002/04/11	06:05:48.63	27.697	56.675	33	4.8	
73	2002/04/13	06:58:23.22	29.016	51.185	33	4.6	
74	2002/04/20	09:35:14.98	27.484	56.630	33	4.7	
75	2002/04/24	19:43:11.09	34.478	47.340	33	4.8	
76	2002/04/30	07:10:52.28	34.460	47.295	33	4.8	
77	2002/05/16	11:00:12.03	29.672	51.706	33	4.8	
78	2002/05/17	15:52:20.92	29.589	51.963	33	4.8	4.0
79	2002/05/28	19:05:32.09	27.719	56.743	59	4.7	
80	2002/06/01	16:12:36.93	29.568	51.226	33	4.9	5.0
81	2002/06/18	21:07:02.54	27.656	54.162	33	4.6	
82	2002/06/19	15:48:25.50	27.344	54.026	33	4.6	
83	2002/07/08	05:42:32.41	31.854	50.637	33	4.6	
84	2002/08/29	09:53:49.77	29.175	51.598	33	4.7	
85	2002/09/09	07:56:51.95	29.447	51.794	33	4.7	
86	2002/10/06	09:51:45.62	28.261	52.826	33	4.6	
87	2002/10/25	21:48:05.82	33.044	48.903	33	4.6	
88	2002/10/27	07:19:10.69	34.263	48.103	33	4.8	
89	2002/12/24	22:17:14.42	34.572	47.415	33	4.7	
90	2002/12/30	18:15:44.57	31.842	49.411	33	4.8	
91	2002/12/31	04:58:17.90	30.905	50.049	33	4.6	
92	2002/12/31	09:06:31.83	34.474	47.426	33	4.8	
93	2002/12/31	22:22:12.98	31.825	49.439	33	4.8	
94	2003/01/01	01:56:48.00	31.801	49.445	33	4.7	
95	2003/01/05	09:48:47.31	33.952	45.478	45	4.6	
96	2003/01/16	02:07:41.90	28.014	55.261	33	4.6	
97	2003/01/16	08:45:05.36	30.510	50.405	33	4.8	
98	2003/04/08	11:48:14.58	32.460	48.037	50	4.6	
99	2003/12/18	07:34:58.17	29.476	50.748	33	4.6	
100	2003/12/25	09:20:43.99	28.552	54.010	33	4.7	
101	2003/12/28	06:42:59.04	28.493	54.120	33	4.6	
102	2003/02/27	01:30:50.03	31.023	49.179	41	4.7	
103	2003/03/08	09:28:03.78	27.983	56.757	33	4.7	
104	2003/03/16	05:42:04.93	28.476	53.028	33	4.6	
105	2003/03/08	22:23:10.63	27.538	54.479	33	4.8	
106							

Table (1) (continue)

No	DATE	ORIGIN TIME	LATITUDE°	LONGITUDE°	DEPTH	Mb	Ms
	YYYY MM DD	HH MM SS.SS			(km)		
107	2003 06 24	13:01:32.83	32.927	49.475	33	4.6	
108	2003 07 11	21:55:44.42	29.472	54.039	10	4.9	
109	2004 08 05	20:41:47.62	31.793	46.129	36	4.6	
110	2003 10 04	00:44:34.61	29.711	51.733	21	4.9	
111	2003 10 05	23:08:34.09	30.157	50.602	33	4.6	
112	2003 10 07	11:04:34.41	28.354	54.352	33	4.6	
113	2004 01 06	02:27:24.08	31.858	49.505	34	4.6	
114	2004 01 06	06:31:15.36	31.904	49.597	61	4.7	
115	2004 01 06	10:03:06.02	31.889	49.526	45	4.6	
116	2004 01 07	04:18:48.69	31.929	49.609	89	4.7	
117	2004 01 18	23:22:34.22	31.891	51.784	63	4.6	
118	2004 01 22	21:19:30.89	29.632	51.222	25	4.7	
119	2004 02 12	09:20:58.46	33.691	45.869	87	4.8	
120	2004 02 15	19:37:39.97	27.770	52.289	65	4.6	
121	2004 02 29	00:22:54.48	32.757	48.114	45	4.6	
122	2004 03 01	16:40:42.80	31.824	49.569	42	4.6	
123	2004 03 02	07:51:43.02	28.942	51.197	10	4.9	
124	2004 03 21	05:04:37.98	32.085	49.395	60	4.6	
125	2004 03 24	18:13:13.92	27.592	56.168	65	4.6	
126	2004 05 24	00:15:00.68	34.086	46.728	44	4.7	
127	2004 06 12	13:24:08.69	33.317	45.905	47	4.7	
128	2004 06 25	14:42:55.51	30.577	50.739	24	4.8	
129	2004 11 19	17:23:40.75	32.061	48.880	10	4.8	
130	2004 11 19	23:49:37.11	32.025	48.856	36	4.6	
131	2004 11 20	02:27:52.22	32.180	48.799	38	4.7	
132	2004 11 20	03:50:45.89	32.064	48.828	26	4.8	
133	2004 11 20	12:06:14.91	32.022	48.794	41	4.7	
134	2004 11 20	14:24:50.63	32.017	48.818	36	5.0	4.1
135	2004 11 21	21:37:24.23	33.301	47.983	10	4.9	
136	2004 11 27	16:12:06.41	33.433	47.945	55	4.6	
137	2005 01 18	16:46:39.50	32.379	49.715	25	4.7	
138	2005 03 03	16:52:59.46	27.277	56.039	35		

Table (2) Earthquake epicenteral data for events located in the Gulf of Aden

No.	DATE	ORIGIN TIME	LATITUDE°	LONGITUDE°	DEPTH	Mb	Ms
	YYYY MM DD	HH MM SS.SS			(km)		
1	1997 03 08	23:29:02.7	11.748	43.263	10	5.1	4.9
2	1997 03 09	13:34:12.9	11.970	43.403	10	4.6	
3	1997 03 09	17:40:18.3	11.696	43.550	10	4.8	5.0
4	1997 03 09	17:41:45.0	11.687	43.412	10	4.7	
5	1997 03 09	19:09:29.7	11.579	43.314	10	4.9	
6	1997 03 11	06:28:44.5	12.084	43.512	10	4.7	
7	1997 03 19	16:34:21.5	13.281	50.059	10		
8	1997 06 12	14:28:23.8	12.704	48.289	10		
9	1997 08 24	09:03:09.0	12.724	47.572	10	4.6	
10	1998 04 24	01:50:31.6	11.757	44.077	10		
11	1998 06 13	23:26:03.4	13.764	50.891	10	5.0	4.6
12	1998 11 23	19:16:45.5	12.347	47.564	10	4.7	
13	1998 11 24	00:50:44.2	12.411	47.569	10	4.8	4.5
14	1999 04 20	18:28:16.5	12.674	47.580	10	4.8	
15	1999 04 20	19:13:20.1	12.984	47.632	10		

Table (2) (continue)

No.	DATE	ORIGIN TIME	LATITUDE°	LONGITUDE°	DEPTH	Mb	Ms
	YYYY/MM/DD	HH:MM:SS.SS			(km)		
16	2000/02/10	01:35:01.96	12.010	45.934	10	5.0	
17	2000/02/14	06:58:27.48	11.904	46.061	10	5.0	
18	2000/02/14	18:20:56.81	11.947	45.947	10	4.6	
19	2000/04/06	14:34:24.85	12.500	47.446	10	4.8	4.4
20	2000/05/02	10:57:28.50	13.450	50.439	33		
21	2000/05/18	21:47:54.21	13.292	50.773	10	4.8	4.3
22	2000/07/25	18:15:27.60	13.578	50.806	10	4.6	
23	2000/08/09	22:08:42.99	11.818	43.651	10	5.0	4.7
24	2000/09/28	13:31:13.77	12.680	48.281	10		
25	2000/10/25	00:30:30.39	13.351	50.764	10	4.7	4.5
26	2000/10/25	00:32:25.56	13.393	50.936	10		
27	2000/10/25	00:35:03.99	13.365	50.817	10		
28	2001/04/23	16:35:35.52	13.274	50.471	10	5.2	4.8
29	2001/06/02	21:02:45.15	12.909	48.429	10		
30	2001/06/15	16:19:07.61	13.903	51.679	10	5.5	5.5
31	2001/08/08	01:10:32.57	13.509	50.846	10	4.6	
32	2001/10/09	03:54:45.47	12.857	49.074	10	4.5	4.6
33	2002/08/10	09:45:41.88	12.128	43.885	10	5.0	4.9
34	2002/10/07	18:10:50.93	13.615	50.922	33	4.8	4.1
35	2003/01/18	04:43:17.10	12.715	48.609	10	4.6	
36	2003/10/11	09:34:15.11	13.958	51.765	10	4.9	
37	2003/11/01	12:04:57.25	13.146	50.493	10	4.7	
38	2004/01/03	23:17:52.48	11.511	43.041	10	4.9	
39	2004/01/04	00:09:46.06	11.640	43.192	10	5.1	4.7
40	2004/04/03	10:10:04.88	13.806	51.549	10	5.0	4.5
41	2004/05/01	14:24:12.65	13.273	52.108	10	4.7	
42	2004/05/24	01:42:36.62	13.310	49.698	10	4.6	
43	2004/11/19	10:39:22.32	13.264	50.717	10	4.7	

Table (3) Love waves attenuation coefficients for Eastern and Southern Arabian Plate compared with the results of Mokhtar (1996)

Period	Eastern Arabia		Southern Arabia		Arabian Plate (Mokhtar, 1996)	
	γL. X 10^{-4}	S. D. X10^{-4}	γL. X 10^{-4}	γL. X 10^{-4}	S. D. X 10^{-4}	γL. X 10^{-4}
11	14.80	1.55	23.23	2.19	20.75	5.15
12	12.80	1.72	21.40	2.37	20.06	5.96
13	10.30	1.62	19.93	2.28	14.64	5.46
14	11.20	1.21	16.09	1.68	15.34	4.51
15	6.28	1.40	9.51	1.82	13.74	4.52
16	3.74	1.23	8.47	1.59	14.03	4.56
17	2.98	1.25	2.75	1.67	3.31	3.79
18	2.68	0.65	3.92	0.97	2.46	2.65
20	2.13	1.07	3.14	1.50	6.27	4.56
22	1.02	0.67	1.13	0.72	3.17	5.03
24	0.46	1.04	0.62	1.16	4.74	4.58
26	1.98	1.37	2.19	1.68	2.38	3.95
28	1.40	0.83	1.53	0.11	2.35	2.35
30	1.66	1.18	1.02	1.38	1.64	3.26
34	1.02	1.09	1.56	1.39	2.75	3.40
38	0.48	1.18	0.03	1.15	2.25	3.65

Table (4). Rayleigh waves attenuation coefficients for Eastern and Southern Arabian Plate compared with the results of Mokhtar (1996)

Period	Eastern Arabia		Southern Arabia		Arabian Plate (Mokhtar, 1996)	
	$\gamma L \times 10^{-3}$	S. D $\times 10^{-3}$	$\gamma L \times 10^{-3}$	$\gamma L \times 10^{-3}$	S. D $\times 10^{-3}$	$\gamma L \times 10^{-3}$
11	14.60	2.03	22.99	2.00	23.63	6.42
12	13.60	2.11	20.02	2.38	20.45	6.83
13	9.84	1.57	19.50	2.31	19.33	6.96
14	9.73	1.92	16.91	1.80	14.55	7.52
15	4.85	1.76	10.58	1.84	13.74	7.22
16	4.98	1.77	9.88	1.65	16.67	9.62
17	5.20	1.19	3.97	3.01	5.79	6.75
18	3.46	1.63	4.44	2.00	4.87	5.53
20	1.29	1.70	5.07	1.45	5.32	4.17
22	2.28	2.12	1.35	2.30	4.98	4.53
24	0.66	1.79	0.267	1.28	2.35	4.15
26	5.18	2.14	4.56	1.74	5.62	5.03
28	1.83	1.04	1.74	1.16	8.04	4.21
30	0.62	1.16	0.10	1.29	4.46	3.45
34	3.37	1.69	1.76	1.22	5.63	4.63
38	2.26	1.61	2.27	1.35	1.85	3.58

Table (5) Q_β^{-1} and Q_α^{-1} for Eastern and Southern Arabian Plate

Depth to the Top	Thickness	$Q_\beta^{-1} \times 10^{-3}$		Q_β		$Q_\alpha^{-1} \times 10^{-3}$		Q_α	
(Km)	(Km)	EAPR	SAPR	EAPR	SAPR	EAPR	SAPR	EAPR	SAPR
0.0	1.0	18.2	26.6	55	38	4.72	6.91	211	145
1.0	1.0	18.0	25.5	56	39	4.66	6.61	215	151
2.0	1.0	17.5	23.0	57	43	4.54	5.96	220	168
3.0	2.0	17.3	21.0	58	48	4.48	5.44	223	184
5.0	2.0	17.9	23.3	56	43	4.62	6.01	216	166
7.0	2.0	18.4	27.6	54	36	4.77	7.15	210	140
9.0	3.0	17.7	29.3	57	34	4.60	7.61	217	131
12.0	3.0	15.8	30.7	63	33	4.08	7.93	245	126
15.0	3.0	12.2	27.1	82	37	2.95	7.01	339	143
18.0	3.0	8.0	18.2	125	55	2.08	4.73	481	211
21.0	4.0	4.5	6.5	222	154	1.17	1.69	855	592
25.0	∞	4.1	3.4	243	294	1.06	0.88	943	113

Table (6) Q_β^{-1} and Q_α^{-1} for the Arabian Plate (Mokhtar, 1996)

Depth to the Top (Km)	Thickness (Km)	Q_β^{-1} X 10-3	Q_α^{-1} X10-3	Q_β	Q_α
0.0	1.0	26.2	6.79	38	147
2.0	2.0	24.0	6.72	42	161
5.0	5.0	21.5	5.57	47	179
10.0	5.0	20.6	5.34	49	187
15.0	5.0	15.0	3.89	67	257
20.0	∞	0.6	0.16	1666	6370

INTRODUCTION

The existence of lateral variations in several physical properties of the crust and upper mantle has been established during the past few decades. Seismic velocity structure and anelastic attenuation are two of these properties. It has been found that, the anelastic attenuation significantly affect the decay of both body and surface waves and that, this decay varies from one region to another in both the crust and upper mantle (e.g. Yacoub and Mitchell, 1977; Mitchell, 1975; Seber and Mitchell, 1992, Mokhtar, 2006). These regional variations may be produced by factors related to the tectonic evolution of the crust and upper mantle. Hence, the knowledge of the distribution of seismic velocity and attenuation within the Earth is very important in seismology.

Attenuation coefficients (γ) and specific quality factors (Q) provide important information regarding the anelasticity of the Earth. Available evidence supports that, the seismic velocity of the crust and upper mantle vary laterally across the Arabian plate (e.g. Mokhtar et al., 2001; and Mokhtar, 2004). However, little is known about the variations of the anelastic attenuation in the region.

The Arabian Peninsula has unusually low Q values (high attenuation) compared to other stable regions. Values of Q for the upper crust vary from 60 along the margin of the Red Sea to 100 in the central part of Arabia (Seber and Mitchell, 1992). Q values of the upper crust in East Arabia range between 60 and 80.

These unusually low values suggest that the observed anelasticity of the Arabian Peninsula is affected by tectonic and epeirogenic activity which has occurred over the past 30 million years in the region.Mokhtar (1996) presented a model for Q_β (Shear wave quality factor) for the Arabian Plate, which indicated that, the attenuation decreases with depth with Q_β increasing from 50 in the upper crust to about 150 or more in the lower crust. More recently, the high attenuation of seismic waves along the crust and upper mantle of western Arabia has been confirmed by Mokhtar (2006) using high quality digital data from two stations lying along a great circle path traversing the Arabian Shield. Almost all previous attenuation studies for the Arabian plate were based on very limited and low quality seismic data. Mokhtar (1996), for example, modified the frequency ratio method and applied it to a limited number of analog observations from RYD and three WWSSN seismic stations (JER, SHI and TAB). His goal was to obtain an estimate for the values of surface waves attenuation coefficients (γ_L and γ_R, Love and Rayleigh wave's attenuation coefficients, respectively) for the Arabian plate, in order to compare it to other tectonic regions in the world. Due to the limited number of observations, he made the assumption that, the Arabian plate has more or less homogenous attenuation properties.

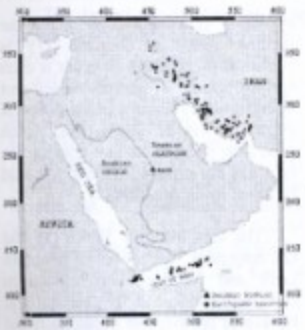

Figure (1) Locations of the earthquakes used in this study. The epicentral parameters of these events are listed in Tables (1) and (2).

In this study, the anelastic attenuation properties variations in the Eastern Arabian Plate region (will be referred to by EAPR from now on) and southern Arabian Plate region (SAPR) are investigated using high quality digital seismic data from 138 earthquakes located in Western Iran, and from 43 earthquakes located in the Gulf of Aden. The digital records of these events derived from RAYN station (A station of the Global SeismicNetwork, GSN), located on the middle part of the Arabian Plate are used.

Tables (1) and (2), Appendex, present the dates, origin times, latitudes, longitudes, depths, and the magnitudes of these events. Their locations are presented in Figure (1). By using these two sets of data, the anelastic attenuation coefficients of surface waves γ_L and γ_R and the Q_β models are determined for the region lying to the east between RAYN station and Western Iran (EAPR), and the region lying between RAYN station and the Gulf of Aden (SAPR). Comparing the results from the two regions will improve our knowledge about the nature and variations of surface wave attenuation properties of the Arabian Plate, as well as the effect of the ongoing tectonic processes in the Red Sea and the Gulf of Aden on these properties.

Determination of γ_L and γ_R

γ_L and γ_R are determined following the method used by Mokhtar (1996), which is a modification of the frequency ratio method. The method can be summarized by the following equation:

$$Ln\left(\frac{|A(\omega)|}{|A(\omega_{40})|}\right) = Ln\left(\frac{|A_o(\omega)|}{|A_o(\omega_{40})|}\right) - |\gamma(\omega) - \gamma(\omega_{40})|r \qquad (1)$$

where:

$A(\omega)$ is the amplitude spectrum of surface waves at the different periods,

$\omega = \dfrac{2\pi}{T}$ is the angular frequency, T is the period.

$A(\omega)$ is the amplitude spectrum of surface waves at a reference period chosen here to be 40 s.

$A_o(\omega)$ is the source spectrum at the different periods which depend on the source mechanism, source depth, and fault orientation.

$A_o(\omega_{40})$ is the value of the source spectrum at 40 s.

$\gamma(\omega)$ is the spatial attenuation coefficient of surface waves.

$\gamma(\omega_{40})$ is the attenuation coefficient at 40 s.

r are the event station epicenteral distances in km.

Equation (1) describes a straight line function with a slope of :

$$b = -[\gamma(\omega) - \gamma(\omega_{40})] \qquad (2)$$

Since $\gamma = \frac{\pi}{TQU}$, where Q is the quality factor, T is the period and U is the group velocity of surface waves, it can be shown as:

$$\gamma(\omega) = b\left[1 + \frac{TU(\omega)}{T_{40}U(\omega_{40})}\right] \qquad (3)$$

The period 40 s is chosen to be the reference period, because the attenuation at this period is governed by properties at depths corresponding to both the lower crust and upper mantle, and hence γ_L and γ_R at 40 s could be considered as the values that represent attenuation deeper than the upper crust and will affect the values of γ_L and γ_R for lower periods. The surface waves group velocities U used in equation (3) are obtained after Mokhtar and Al-Saeed (1994).

The method was applied by Mokhtar (1996) to data from RYD station and a number of WWSSN stations located along the northern and eastern boundaries of the Arabian plate. The original frequency ratio method is used for a certain event and a number of stations. However, due to the lack of data from more than one station, an alternative way to use this method is to apply it to a number of events recorded by one or more stations as long as the spectral ratio in equation (1) is evaluated for a particular event at each specific station. By plotting the left part of equation (1) versus r of the different events, b can be determined, which equals the slope of the best least square fitting of the straight line, and γ could be found using equation (3).

The data listed in Tables (1) and (2), Appendex, are processed to obtain Love and Rayleigh wave spectrum from each earthquake. The vertical and transverse components of all the listed events were derived from RAYN station records. The vertical component (BHZ) and the two horizontal components (BHN and BHE) of each event were corrected for instrument response and filtered using a band-pass Butterworth filter with corner frequencies at 0.01 Hz and 1.0 Hz. Instrument response corrections were performed using the poles and zeros values for each component. The two horizontal components were then rotated to produce radial and transverse (Love) components. The time series of each component was transformed using the Fast Fourier Transform (FFT) and γ_R is computed from the vertical components, while γ_L is computed from the transverse components. For each component, the corrected spectrum was interpolated using the cubic spline interpolation at a spectral interval of 1 second period.

Figures (2) and (3) present an example of the least square regression analysis performed on the determined amplitude spectrum for both the Love and Rayleigh waves, respectively. It is clearly evident that, b for EAPR is less than that for SAPR for both phases.

The dashed straight lines in these figures are from Mokhtar (1996). Tables (3) and (4), Appendex, present γ_L and γ_R values for regions, as well as γ_L and γ_R determined by Mokhtar (1996) for comparison. It is evident from Figure (4) that, γ_L and γ_R values for Southern Arabia are comparable to those of Mokhtar (1996). It is also evident that, the attenuation of surface waves in EAPR at periods less than 16 s is less than that for SAPR. In EAPR, γ_L decreases from 14.6 X 10^{-4} Km^{-1} at 11 s to 1.29 X 10^{-4} Km^{-1} at 18 s. In SAPR, γ_L decreases from 22.09 X 10^{-4} Km^{-1} to 5.07 X 10^{-4} Km^{-1} at 20 s.

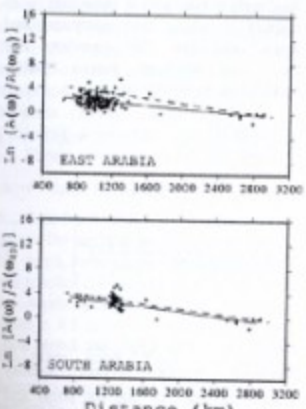

Figure (2) Least squares regression analysis of the amplitude ratio data for Love wave for EAPR and SAPR. Points at distances greater than 1600 km and the least squares fit represented by the dashed line are from Mokhtar (1996).

At periods longer than 20 s, γ_L oscillates between a maximum of about 4.56 to 5.18 X 10^{-4} Km^{-1} and a minimum of 0.10 to 0.62 X 10^{-4} Km^{-1}.

Similar conclusion can be drawn for γ_R, which decreases from 14.80 10^{-4} Km^{-1} at 11 s to 2.13 X 10^{-4} Km^{-1} at 20 s in EAPR, while it decreases from 23.23 X 10^{-4} Km^{-1} at 11 s to 3.14 X 10^{-4} Km^{-1} at 20 s. Beyond 20 s period, γ_R ranges between 0.48 and 1.98 X 10^{-4} Km^{-1} for EAPR, and it varies from 0.03 to 2.19 X 10^{-4} Km^{-1} for SAPR. The scatter of the data at periods longer than 20 s is less pronounced for Rayleigh wave's attenuation coefficients than for Love waves.

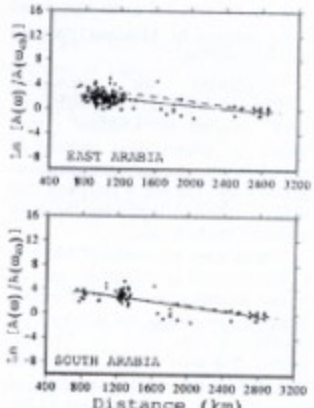

Figure (3) Least squares regression analysis of the amplitude ratio data for Rayleigh wave for EAPR and SAPR. Points at distances greater than 1600 km and the least squares fit represented by the dashed line are from Mokhtar (1996).

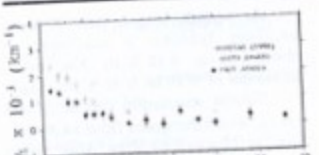

Figure (4) Comparison between γ_L and γ_R for east and south Arabia and those obtained by Mokhtar(1996) for the Arabian Plate.

Comparing the attenuation coefficients obtained in this study with those obtained by Mokhtar (1996) shows the improvement attained in evaluating the attenuation coefficients in this study. The use of sufficient data points has led to improving the error estimates for each value.

In addition, the results of Mokhtar (1996) revealed the abrupt decrease of γ_L and γ_R values at 17 s. This sudden decrease was clearly the result of the insufficient data used by Mokhtar (1996). The most important result of this study is the obvious variations of γ_L and γ_R between EAPR and SAPR, which has not been detected previously in the study of Mokhtar (1996).

Inversion for Q_β

Once the Love and Rayleigh waves attenuation observations have been made, it is necessary to invert them for attenuation as a function of depth.

The inverse problem for obtaining the depth dependence of Q from surface waves has been discussed by a number of authors including Anderson, et al. (1965), Lee and Solomon (1975 and 1978), and Cheng and Mitchell (1981). Mokhtar (1996) followed Anderson, et al. (1965) method to determine Q_β^{-1} using the determined γ_L and γ_R. The quality factor for surface waves can be determined from the quality factors of body waves and the partial derivatives of Love and Rayleigh waves phase velocities with respect to shear and compressional wave velocities. The equations for Love and Rayleigh waves quality factors can be written as:

$$Q_L^{-1} = \sum_{k=1}^{N} \frac{\beta_k}{C_L} \frac{\partial C_L}{\partial \beta_k} Q_{\beta_k}^{-1} \qquad (4)$$

$$Q_R^{-1} = \sum_{k=1}^{N} \left[\frac{\beta_k}{C_R} \frac{\partial C_R}{\partial \beta_k} Q_{\beta_k}^{-1} + \frac{\alpha_k}{C_R} \frac{\partial C_R}{\partial \alpha_k} Q_{\alpha_k}^{-1} \right] \qquad (5)$$

where; Q_L^{-1} and Q_R^{-1} are Love and Rayleigh waves inverse quality factors, β and α are the shear and compressional waves velocities; C_L and C_R are the Love and Rayleigh waves phase velocities; and k is the layer index.

Assuming that, there are no losses under compression for an isotropic material, the relationship between P-wave and S-wave attenuation is given by Anderson, et al., (1965), as follow:

$$Q_\beta^{-1} = \frac{4}{3}\left(\frac{\beta}{\alpha}\right)^2 Q_\alpha^{-1} \qquad (6)$$

Thus, the Love and Rayleigh wave's attenuation coefficients have been inverted to obtain Q_β^{-1}, as a function of depth using equations (4) and (5). Perturbations to Q_β^{-1} values are calculated using a stochastic inverse scheme, as discussed by Wiggins (1972), and Lee and Solomon (1975).

The results of the inverted Q_β^{-1} model for both EAPR and SAPR are shown in Figure (5) and are listed in Table (5), Appendex. The shear-wave attenuation models for both regions are compared with the results obtained by Mokhtar (1996), which are listed in Table (6), Appendex, and are plotted on Figure (5). The inversion results show that, in EAPR, Q_β^{-1} values decrease from 18.2 X 10^{-3} immediately below the surface to 17.3 X 10^{-3} at 3 km depth. It increases below this depth and reaches a value of 18.4 X 10^{-3} at 7 km depth. Below 7 km, it decreases again to 4.1 X 10^{-3} at 25 Km depth. On the other hand, Q_β^{-1} for SAPR decreases from 26.6 X 10^{-3} near the surface to 21 X 10^{-3} at 3 Km depth. It increases below 5 Km from 21. X 10^{-3} to 30 X 10^{-3} at 12 Km depth. Q_β^{-1} starts to decrease again from 30 X 10^{-3} to 3.4 X 10^{-3} at 25 Km depth.

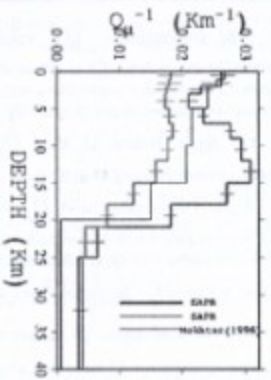

Figure (5) Q_μ^{-1} models for EAPR (Blue) and SAPR (Red) obtained from inversion of measured γ_L and γ_R. The black line represents the model for the Arabian plate from Mokhtar (1996).

Comparing the inverted Q_β^{-1} with those obtained by Mokhtar (1996) indicates that, EAPR is characterized by lower Q_β^{-1} than that of the Arabian Plate, while SAPR has similar Q_β^{-1} values down to about 2 Km depth, below which Q_β^{-1} of SAPR is lower than the Arabian Plate in a 3 Km thick layer. At depths lower than 5 Km, Q_β^{-1} of SAPR is much higher than those values of Mokhtar (1996) up to the base of the upper crust.

The corresponding Q_β values for EAPR range from 54 to 58 in the upper 12 Km of the crust. It increases from 63 below this depth to reach 82 at 15 km depth. Below 15 Km, Q_β increases from 125 to 243 at 25 Km depth. On the other hand, Q_β for SAPR increases from 38 immediately below the surface to 48 at 3 Km depth. Below 5 Km, Q_β decreases from 48 to 33 at 12 Km depth. Q_β starts to increase again below 15 Km from 33 to reach 55 at 18 Km. Below the last depth, Q_β increases to 154 and reaches 294 at 25 km depth. In general, Q_β for EAPR are higher than those for SAPR, indicating lower attenuation in EAPR than in SAPR. Equation (6) is used to compute Q_α^{-1} in Tables (5) and (6), Appendex, and the inverted models were used to compute the theoretical γ_L and γ_R, which are plotted with observed data for comparison in Figures (6) and (7). Good agreement between the computed and observed γ_L and γ_R values has been obtained.

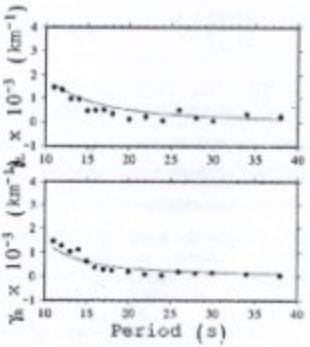

Figure (6) Calculated γ_L and γ_R (curve) compared with observed values for EAPR.

Discussions and Conclusions

Seber and Mitchell (1992) presented Q_β values for the upper crust of the Arabian Peninsula that found to vary from 60 along the margin of the Red Sea to 100-150 at the central part of the peninsula, to 65-80 at the eastern folded region.

Mokhtar (1987) found that, Q_β in the Arabian shield increases gradually from 30 in the upper 50 meters to 150 at about 0.5 km depth. These values were obtained from surface waves data using Saudi Arabia deep seismic refraction profile, which exclusively traverses, for 1000 km, the Arabian shield in a NE-SW direction. It should be noted that, the work of Mokhtar (1987) also showed lateral variations in the attenuation across the shield. Ghalib (1932) noted similar pattern of lateral variations in attenuation.

He found that, the Coda Q values increase from 163 at the western part of Arabia to 286 at the eastern part of Arabia indicating that, the Arabian shield Q gradually increases eastward, but decreases abruptly toward the Red Sea to the west.

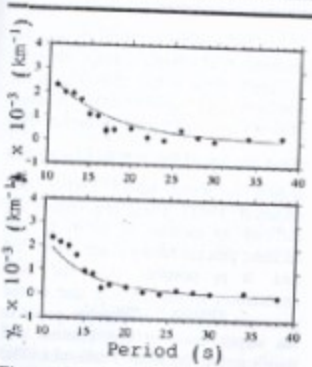

Figure (7) Calculated γ_L and γ_R (curve) compared with observed values for SAPR.

Mokhtar (1995) used Q_β of 75 for the upper 25 km of the crust to produce synthetic seismograms that match observations along a path traversing the Arabian platform from Western Iran to RYD station close to RAYN station. Also, Mokhtar (2006) found that, the surface wave attenuation in the crust and upper mantle at the Southwestern Arabian Peninsula and the Southern Red Sea is extremely high. He attributed the high attenuation to the on going tectonic process in the Red Sea and the Afar depression.

Recently, Cong and Mitchell (1998) obtained shear Q models for the Turkish and Iranian Plateaus (Region 1), areas surrounding including the Black and Caspian Seas (Region 2) and the Arabian Peninsula (Region 3). They found that, Q's for the upper 10 km of the crust are 63, 71 and 201 for Regions 1, 2 and 3, respectively. Crustal Q's at 30 km depth for the three regions are 51, 71, and 134. They attributed these low values of Q to fluids residing in faults, cracks and permeable rocks at the lower crustal depths, as well as the upper crustal depths due to intense deformation at all depths in the Middle Eastern crust.

The results of this study are in good agreement with those of Seber and Mitchell (1992) and of Mokhtar (1995). The high value of Q_β obtained by Cong and Mitchell (1998) for the upper 10 km of the crust of the Arabian Peninsula may reflect an average of Q_β for the upper crust of the Arabian Plate, while Q_β values obtained in this study represent the average for the upper crust of two distinct geological units, namely the eastern folded regions known as the Arabian platform, and the southern part of the Arabian shield.

In laboratory study pertaining to attenuation at crustal depths, Housley, et al. (1974) showed that, only a few mono-layer of water absorbed on pore surfaces of granite would drastically reduce Q. Wrinkler and Nur (1979) measured the attenuation of sandstone at various degrees of saturation and found that, the energy loss by fluid flow is likely to be the dominant form of seismic energy loss, at least in the shallow crust. In a later experimental study, Wrinkler and Nur (1982) found that, the partial water saturation significantly increases the attenuation of both compressional and shear waves relative to that in dry rock.

Mitchell (1975) proposed that, the regional crustal Q variations result from lateral variations of the volume of interstitial fluids, possibly water of